Published in IET Radar, Sonar and Navigation
Received on 13th December 2011
Revised on 10th March 2012
doi: 10.1049/iet-rsn.2011.0394

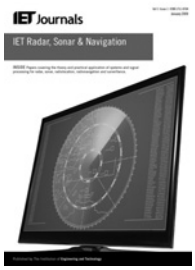

ISSN 1751-8784

Receivers' positioning in multiple-input multiple-output digital video broadcast-terrestrial-based passive coherent location

M. Radmard B.H. Khalaj M.M. Chitgarha M. Nazari Majd M.M. Nayebi

Department of Electrical Engineering, Sharif University of Technology, Tehran, Iran
E-mail: radmard@ee.sharif.ir

Abstract: Using multiple illuminators of opportunity at the transmit side and multiple antennas at the receiver side in a passive coherent location (PCL) scheme is expected to improve the detection performance. However, in such multiple-input multiple-output (MIMO) configuration choosing the position of the receivers is an obstacle that can have significant influence on the resulting performance. In this study, the authors consider the case of digital video broadcast (DVB)-T stations as non-cooperative transmitters and introduce a procedure based on the probability of missed detection to properly place receive antennas in a MIMO digital video broadcasting (DVB)-T based PCL configuration.

1 Introduction

1.1 Passive coherent location

As a low-cost technology, passive coherent location (PCL) has attracted much attention in recent years. Different kinds of available signals have been investigated for such use, for example, FM [1–3], wireless LAN transmissions [4], analogue TV [5, 6], digital TV [7–10], satellite [11] and GSM [12–14] systems. New digital signals, such as digital audio/video broadcast, are excellent candidates for such purpose [15–17], as they are widely available and can be easily decoded.

Traditionally the object's range is measured by comparing the time of transmit and receive pulses. However, such information is not directly available in the case of PCL. Instead, two sets of antennas are used, one for receiving the signal directly from its main source (reference antenna) and another one for collecting reflections arriving from the objects that are to be detected (reflection antenna). Fig. 1 depicts the overall structure of this passive scheme.

In such scenarios, detection is done through computation of cross ambiguity function (CAF), as given in (1), which is a criterion of how much correlation exists between reference and reflected signals. A given CAF's peak in a range–Doppler cell is a representative of a potential object in that range and Doppler frequency

$$|\chi(\tau, \nu)|^2 = \left| \int_T r(t) s^*(t-\tau) \mathrm{e}^{-\mathrm{j}2\pi\nu t} \right|^2 \quad (1)$$

where $r(t)$ is the received signal, $s(t)$ is the reference signal, ν is the Doppler shift, τ is the delay shift and T is the integration interval.

1.2 Multiple-input multiple output (MIMO) localisation

After a spark in communication in 1998 [18] that developed MIMO communication, recently there has been a great attention towards MIMO in localisation. Researchers have studied this topic from several points of view. Generally, MIMO localisation is divided into two categories: with use of widely separated antennas and use of collocated antennas [19, 20].

In the case of widely separated antennas, we use multiple transmitters and multiple receivers that are widely separated in order to detect the objects of interest. The difference of this approach with multistatic cases is in its jointly processing nature. As shown in [19] the concepts of spatial diversity and multiplexing gain emerge here in a dual manner to the MIMO communication. The main point is that, by looking at an object from different angles, the probability of missed detection decreases, a concept known as spatial diversity in MIMO communication. On the other hand, in the case of collocated antennas, transmitters and receivers instead of being widely separated, are collocated. Such configuration is similar to phased array schemes, however, here the signals emitted by each antenna can be totally uncorrelated with each other.

The studies have shown that we can have enhanced detection performance (diversity gain) [21, 22] and high-resolution object localisation (spatial multiplexing gain) [23] with a widely separated antennas scheme. Similarly, significantly improved parameter identifiability [24], direct applicability of adaptive arrays for target detection and parameter estimation [25] and much enhanced flexibility for transmit beampattern design [26, 27] is obtained by using the collocated antennas scheme.

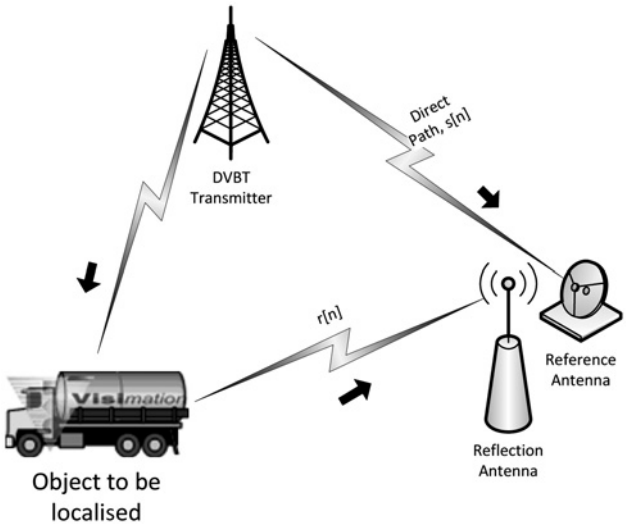

Fig. 1 *Structure of a passive scheme*

1.3 MIMO PCL, a new concept

As described earlier, it is possible to achieve the benefits of both MIMO and PCL by using multiple receivers to detect targets illuminated by multiple non-cooperative transmitters, even when the illuminators are transmitting different signals (e.g. a broadcasting FM radio station with a GSM base station).

Although MIMO localisation is a well-known technique (e.g. [19, 22, 24–28]), the problem of positioning transmit and receive antennas has not been properly addressed in the literature [29, 30]. In this paper, we introduce a procedure for proper placement of receive antennas based on improving the probability of missed detection. It should be noted that choosing the positions of transmit antennas is not addressed since in the case of PCL, the illuminators of opportunity are already installed in the environment and there is not much control over their location. In the following, we simulate the case of a 2×2 digital video broadcast (DVB)-T-based MIMO PCL and introduce a technique for finding the position of the receive antennas.

The rest of this paper is organised as follows. Section 2 develops the structure of the detector for the DVB-T-based MIMO PCL and the probability of missed detection is analysed to derive a closed form. Then, in Section 3, it is used as a criterion for placing the receive antennas. The effect of increasing the number of receive antennas on system performance is analysed in Section 4. Joint performance of receivers is studied in Section 5, and finally, Section 6 concludes the paper.

2 Detection in the DVB-T-based MIMO PCL

In the case of DVB-T signal, the transmitted signals from all stations are exactly the same (a concept referred to as an SFN – single frequency network– of DVB-T transmitters), so that the echoes of the targets illuminated by the transmitters collected by each receiver all have the same structure.

Assume that there are M illuminators of opportunity (e.g. broadcasting DVB-T signals in a single frequency network), a single receiver (including a reference and a reflection antenna) and, an object to be localised. For simplification, we have assumed that the object to be localised has no Doppler, although this assumption is not critical in our derivations. Indeed, when we have Doppler effect, the received signal will have a Doppler shift. As the receiver performs match filtering on the received signal, it is filtered with different copies of the signal with different Doppler values. Consequently, the Doppler will be removed and there will be no need to consider it separately in this manuscript.

The reflection antenna is assumed to be omnidirectional, collecting signals arriving from all directions. At the receiver side, after direct path interference cancellation [31], the signal is passed through a CAF processor to obtain the delays and Doppler frequencies of different echoes collected from the objects to be localised. The threshold at the output of CAF processor for declaring that an object is detected is determined by the desired false alarm rate (P_{fa}). In the case of MIMO PCL, the signal received at a receive antenna is presented by (2)

$$r(t) = \sqrt{\frac{E_{\text{t}}}{L}} \sum_{i=1}^{M} \frac{\alpha_i}{r_{1i} r_{2i}} s(t - \tau_i) + n(t) \tag{2}$$

where $s(t)$ is the transmitted signal, r_{1i} and r_{2i} are the distance from the transmitter to the target and the distance from the target to the receiver respectively, M is the number of illuminators, α_i is the cross-section gain of the object illuminated by the signal transmitted from the ith transmitter, E_{t} is the energy of the transmitted signal, L is the channel loss and τ_i denotes its delay.

We define the probability of missed detection (P_{M}) as the probability that we miss all echoes of the desired object. It should be noted that in order to find the location of the object by one receiver, we should have at least three echoes from three transmitters in the two-dimensional plane. However, the reason that we do not consider the case of detecting one or two echoes as missed detection is that we can design the detector such that after detecting one or two echoes, the threshold can be reduced adaptively in order to detect sufficient number of echoes (in this case three). Although by such approach P_{fa} would increase, the data association algorithm we have developed in [32], used to associate these echoes to targets, will eliminate such false echoes. Another reason is that we can localise the object by other techniques such as direction-of-arrival estimation after detecting it at an acceptable P_{M} level. More importantly, data fusion schemes can be adopted to localise objects by multiple receivers, in which case it is not required to have three echoes at each receiver.

2.1 Problem formulation

Next, we explore the probability of missed detection in MIMO PCL by computing the detection probability.

First, our objective is to find the optimum position only for the first receive antenna. Therefore we assume the receiver is placed at $\tilde{X}$, an arbitrary place in the region of interest. For the target located at position $\tilde{Y}$, the echo of the ith transmitter will be missed with the probability P_{M}^{i}. As described earlier, we have

$$P_{\text{M}} = \prod_{i=1}^{M} P_{\text{M}}^{i} \tag{3}$$

In other words, we consider a target totally missed, if we do not detect any of its echoes.

doi: 10.1049/iet-rsn.2011.0394

Now, consider the hypothesis in which we assume a target exists in the specific bistatic range corresponding to the position $\tilde{Y}$. The bistatic range of the echo from the ith transmitter will be

$$r_i = r_{1i} + r_{2i} \tag{4}$$

where r_{1i} and r_{2i} represent the target–transmitter and target–receiver distance, respectively. However, existence of the target in this cell is a random process with unknown probability. We use the Neyman–Pearson hypothesis test because priori probabilities are unknown. So we will obtain the likelihood ratio to compare it with a threshold (η). The hypotheses are shown below

$$\begin{aligned} &\mathcal{H}_0: \boldsymbol{y} = \boldsymbol{n} \\ &\mathcal{H}_1: \boldsymbol{y} = \boldsymbol{n} + c\boldsymbol{s} \end{aligned} \tag{5}$$

where $\boldsymbol{s}$ and $\boldsymbol{n}$ are signal and noise vectors with length m, respectively. As shown in [8], because of highly randomised nature of DVB-T symbols, the echo of target in other bistatic range cells behave as weak uncorrelated noise that can be ignored in this model.

In the absence of a target, the received signal is white noise with independent samples with a jointly distributed function as follows

$$f_N(\boldsymbol{n}) = \prod_{i=1}^{m} \frac{1}{\sqrt{2\pi}\sigma_n} \mathrm{e}^{-(n_i^2/2\sigma_n^2)} = \frac{1}{\left(\sqrt{2\pi}\sigma_n\right)^m} \mathrm{e}^{-\left(\sum_{i=1}^{m} n_i^2/2\sigma_n^2\right)} \tag{6}$$

where σ_n^2 is the power of receiver noise.

However, if the target exists in the given bistatic range cell, it reflects the transmitted signal in proportion to its RCS. We assume its radar cross section (RCS) follows the Swerling I model (also called Rayleigh scatter). If σ^2 represents RCS, the distribution function of σ is

$$f_\sigma(\sigma) = \frac{\sigma}{\sigma_t^2} \mathrm{e}^{-(\sigma^2/2\sigma_t^2)} \tag{7}$$

where σ_t^2 is the RCS average value.

In (5) the coefficient c (the gain experienced by the signal from the transmitter to the receiver) is

$$c = \frac{\sigma v}{r_{1i} r_{2i}} \tag{8}$$

where

$$v = \sqrt{\frac{P_\mathrm{t} G_\mathrm{t} G_\mathrm{r} I_\mathrm{p}}{L_\mathrm{c} L_\mathrm{r}}} \tag{9}$$

In the above equation, P_t is the transmitted power, G_t and G_r are the transmitting and receiving antenna gains respectively, I_p is the processing gain at the receiver, L_c is the scattering loss and L_r is the receiver loss.

Without loss of generality, we assume that $\|\boldsymbol{s}\| = 1$

$$||\boldsymbol{s}||^2 = \sum_{i=1}^{m} s_i^2 = 1 \tag{10}$$

The distribution function of c results from the distribution function of σ. Using (7) and (8), we have

$$f_\mathrm{C}(c) = \frac{f_\sigma(\sigma)}{|\partial c/\partial\sigma|} = \left(\frac{r_{1i} r_{2i}}{v}\right)\left(\frac{\sigma}{\sigma_t^2} \mathrm{e}^{-(\sigma^2/2\sigma_t^2)}\right)\Bigg|_{\sigma=(r_{1i} r_{2i} c/v)} \tag{11}$$

$$f_\mathrm{C}(c) = \left(\frac{r_{1i} r_{2i}}{v\sigma_t}\right)^2 c \mathrm{e}^{-(1/2)(r_{1i} r_{2i}/v\sigma_t)^2 c^2} \tag{12}$$

From (5) and (6)

$$f_{\boldsymbol{Y}}(\boldsymbol{y}|H_0) = f_N(\boldsymbol{y}) = \frac{1}{\left(\sqrt{2\pi}\sigma_n\right)^m} \mathrm{e}^{-(1/2\sigma_n^2)\sum_{i=1}^{m} y_i^2} \tag{13}$$

We also obtain

$$f_{\boldsymbol{Y}}(\boldsymbol{y}|H_1) = \int_0^\infty f_{\boldsymbol{Y}}(\boldsymbol{y}|C = c, H_1) f_\mathrm{C}(c)\, \mathrm{d}c \tag{14}$$

For H_1 hypothesis

$$\boldsymbol{y} = \boldsymbol{n} + c\boldsymbol{s} \tag{15}$$

$$\begin{aligned} f_{\boldsymbol{Y}}(\boldsymbol{y}|C = c, H_1) &= f_N(\boldsymbol{y} - c\boldsymbol{s}) \\ &= \frac{1}{\left(\sqrt{2\pi}\sigma_n\right)^m} \mathrm{e}^{-(1/2\sigma_n^2)\sum_{i=1}^{m} (y_i - cs_i)^2} \end{aligned} \tag{16}$$

(see (17) and (18))

$$f_{\boldsymbol{Y}}(\boldsymbol{y}|H_1) = a_0 \int_0^\infty c \mathrm{e}^{-a_1^2 c^2 + a_2 c - a_3}\, \mathrm{d}c \tag{19}$$

where

$$a_0 = \frac{r_{1i}^2 r_{2i}^2}{v^2 \sigma_t^2 \left(\sqrt{2\pi}\sigma_n\right)^m} \tag{20}$$

$$a_1^2 = \frac{1}{2\sigma_n^2} \sum_{i=1}^{m} s_i^2 + \frac{1}{2}\left(\frac{r_{1i} r_{2i}}{v\sigma_t}\right)^2 \tag{21}$$

$$f_{\boldsymbol{Y}}(\boldsymbol{y}|H_1) = \int_0^\infty \frac{1}{\left(\sqrt{2\pi}\sigma_n\right)^m} \mathrm{e}^{-(1/2\sigma_n^2)\sum_{i=1}^{m} (y_i - cs_i)^2} \left(\frac{r_{1i} r_{2i}}{v\sigma_t}\right)^2 c \mathrm{e}^{-(1/2)(r_{1i} r_{2i}/v\sigma_t)^2 c^2}\, \mathrm{d}c \tag{17}$$

$$= \frac{r_{1i}^2 r_{2i}^2}{v^2 \sigma_t^2 \left(\sqrt{2\pi}\sigma_n\right)^m} \int_0^\infty c \mathrm{e}^{-c^2((1/2\sigma_n^2)\sum_{i=1}^{m} s_i^2 + (1/2)(r_{1i} r_{2i}/v\sigma_t)^2) + c((1/2\sigma_n^2)\sum_{i=1}^{m} y_i s_i) - (1/2\sigma_n^2)\sum_{i=1}^{m} y_i^2}\, \mathrm{d}c \tag{18}$$

According to (10)

$$a_1^2 = \frac{1}{2\sigma_n^2} + \frac{1}{2}\left(\frac{r_{1i}r_{2i}}{v\sigma_t}\right)^2 \tag{22}$$

$$a_2 = \frac{1}{\sigma_n^2}\sum_{i=1}^{m} y_i s_i \tag{23}$$

$$a_3 = \frac{1}{2\sigma_n^2}\sum_{i=1}^{m} y_i^2 \tag{24}$$

$$\begin{aligned} f_{\boldsymbol{Y}}(\boldsymbol{y}|H_1) &= a_0\int_0^\infty c\mathrm{e}^{-a_1^2c^2+a_2c-a_3}\,\mathrm{d}c \\ &= a_0\int_0^\infty c\mathrm{e}^{-(a_1c-(a_2/2a_1))^2+((a_2^2/4a_1^2)-a_3)}\,\mathrm{d}c \qquad (25) \\ &= a_0\mathrm{e}^{(a_2^2/(4a_1^2))-a_3}\int_0^\infty c\mathrm{e}^{-(a_1c-(a_2/2a_1))^2}\,\mathrm{d}c \\ &= \frac{a_0}{a_1^2}\mathrm{e}^{(a_2^2/4a_1^2)-a_3}\left(\int_{-(a_2/2a_1)}^\infty x\mathrm{e}^{-x^2}\,\mathrm{d}x\right. \\ &\quad \left. +\frac{a_2}{2a_1}\int_{-(a_2/2a_1)}^\infty \mathrm{e}^{-x^2}\,\mathrm{d}x\right) \qquad (26) \\ &= \frac{a_0}{a_1^2}\mathrm{e}^{(a_2/2a_1)^2-a_3} \\ &\quad \times\left(-\frac{1}{2}\mathrm{e}^{-x^2}\Big|_{-(a_2/2a_1)}^\infty + \frac{a_2}{2a_1}\frac{\sqrt{2\pi}}{\sqrt{2}}Q\left(-\frac{\sqrt{2}a_2}{2a_1}\right)\right) \qquad (27) \end{aligned}$$

where

$$Q(x) = \int_x^\infty \frac{1}{\sqrt{2\pi}}\mathrm{e}^{-(x'^2/2)}\,\mathrm{d}x' \tag{28}$$

so

$$f_{\boldsymbol{Y}}(\boldsymbol{y}|H_1) = \frac{a_0}{a_1^2}\mathrm{e}^{(a_2/2a_1)^2-a_3}\left(\frac{1}{2}\mathrm{e}^{-(a_2/2a_1)^2} + \frac{a_2\sqrt{\pi}}{2a_1}Q\left(-\frac{a_2}{a_1\sqrt{2}}\right)\right) \tag{29}$$

$$= \frac{a_0}{2a_1^2}\mathrm{e}^{-a_3}\left(1+\frac{a_2\sqrt{\pi}}{a_1}Q\left(-\frac{a_2}{a_1\sqrt{2}}\right)\mathrm{e}^{(a_2/2a_1)^2}\right) \tag{30}$$

The likelihood ratio is defined below

$$L(\boldsymbol{y}) = \frac{f_{\boldsymbol{Y}}(\boldsymbol{y}|H_1)}{f_{\boldsymbol{Y}}(\boldsymbol{y}|H_0)} \tag{31}$$

For H_0 hypothesis, we can write

$$\begin{aligned} f_{\boldsymbol{Y}}(\boldsymbol{y}|H_0) &= \frac{1}{\left(\sqrt{2\pi}\sigma_n\right)^m}\mathrm{e}^{-(1/2\sigma_n^2)\sum_{i=1}^m y_i^2} \\ &= \frac{1}{\left(\sqrt{2\pi}\sigma_n\right)^m}\mathrm{e}^{-a_3} \qquad (32) \end{aligned}$$

By using (30)–(32) and simplifying the likelihood ratio, we have

$$L(\boldsymbol{y}) = \frac{a_0\left(\sqrt{2\pi}\sigma_n\right)^m}{2a_1^2}\left(1+\frac{a_2\sqrt{\pi}}{a_1}Q\left(-\frac{a_2}{a_1\sqrt{2}}\right)\mathrm{e}^{(a_2/2a_1)^2}\right) \tag{33}$$

In the above equation, the two terms $Q(-(a_2a_1\sqrt{2}))$ and $\mathrm{e}^{(a_2/2a_1)^2}$ increase by increasing a_2. This fact results in increasing $L(\boldsymbol{y})$ by increasing a_2. Therefore according to the Neyman–Pearson lemma

$$L(\boldsymbol{y}) \underset{H_0}{\overset{H_1}{\gtrless}} \eta_1 \tag{34}$$

so

$$a_2 \underset{H_0}{\overset{H_1}{\gtrless}} \eta_2 \tag{35}$$

$$\sum_{i=1}^{m} y_i s_i \underset{H_0}{\overset{H_1}{\gtrless}} \eta \tag{36}$$

This equation shows that if we use the matched filter at the receiver, we have optimal efficiency in the detection of the target placed at a specific bistatic range cell. Subsequently, η must be determined to achieve the desired false alarm probability.

For the H_0 hypothesis

$$\boldsymbol{y} = \boldsymbol{n} \tag{37}$$

The matched filter output for this hypothesis is defined below

$$E = \sum_{i=1}^{m} n_i s_i \tag{38}$$

For E, we have

$$f_E(e) = \frac{1}{\sqrt{2\pi}\sqrt{\sigma_n^2\sum_{i=1}^m s_i^2}}\mathrm{e}^{-\left(e^2/\left(2\sigma_n^2\sum_{i=1}^m s_i^2\right)\right)} \tag{39}$$

From (10) and (39)

$$f_E(e) = \frac{1}{\sqrt{2\pi}\sigma_n}\mathrm{e}^{-(e^2/2\sigma_n^2)} \tag{40}$$

False alarm probability is obtained from (36) and (40) as follows

$$P_{\mathrm{fa}} = \Pr\left\{\sum_{i=1}^{m} y_i s_i > \eta | H_0\right\} \tag{41}$$

$$= \Pr\left\{\sum_{i=1}^{m} n_i s_i > \eta\right\} \tag{42}$$

$$= \Pr\{e > \eta\} = Q\left(\frac{\eta}{\sigma_n}\right) \tag{43}$$

doi: 10.1049/iet-rsn.2011.0394

By substituting α instead of p_{fa}, the threshold value η is obtained

$$\alpha = Q\left(\frac{\eta}{\sigma_n}\right) \tag{44}$$

$$\eta = \sigma_n Q^{-1}(\alpha) \tag{45}$$

Now, assume the target is placed in this cell

$$\boldsymbol{y} = \boldsymbol{n} + c\boldsymbol{s} \tag{46}$$

The matched filter output for this hypothesis is defined as

$$F = \sum_{i=1}^{m} (n_i + cs_i)s_i = \sum_{i=1}^{m} n_i s_i + \sum_{i=1}^{m} cs_i^2 = E + G \tag{47}$$

$$G = \sum_{i=1}^{m} cs_i^2 = \left(\sum_{i=1}^{m} s_i^2\right)c \tag{48}$$

Considering (10), we obtain

$$G = c \tag{49}$$

and

$$f_G(g) = f_C(g) \tag{50}$$

$$f_G(g) = g\left(\frac{r_{1i}r_{2i}}{v\sigma_t}\right)^2 \mathrm{e}^{-(1/2)(r_{1i}r_{2i}/v\sigma_t)^2 g^2} \tag{51}$$

The detection probability according to (46) and (47) is obtained as follows

$$P_{\text{d}}^i = \Pr\left\{\sum_{i=1}^{m} y_i s_i > \eta | H_1\right\} = \Pr\left\{\sum_{i=1}^{m} (n_i + cs_i)s_i > \eta\right\} \tag{52}$$

$$= \Pr\{F > \eta\} = \Pr\{E + G > \eta\}$$

$$= \int \Pr\{G > \eta - \theta | E = \theta\} f_E(\theta)\,\mathrm{d}\theta \tag{53}$$

The independence of noise and RCS results in the independence of E and G. As a result, we have

$$\Pr\{G > \eta - \theta | E = \theta\} = \Pr\{G > \eta - \theta\} \tag{54}$$

By computing the cumulative distribution function for Rayleigh distribution, we obtain

$$\Pr\{G > \eta - \theta\} = \mathrm{e}^{-((\eta-\theta)^2/2\sigma_1^2)}, \quad \theta < \eta \tag{55}$$

where

$$\sigma_1 = \frac{v\sigma_t}{r_{1i}r_{2i}} \tag{56}$$

Using (53) and (55) we have

$$P_{\text{d}}^i = \int_{-\infty}^{\eta} \mathrm{e}^{-((\eta-\theta)^2/2\sigma_1^2)} \frac{1}{\sqrt{2\pi}\sigma_n} \mathrm{e}^{-(\theta^2/2\sigma_n^2)}\,\mathrm{d}\theta \tag{57}$$

$$P_{\text{d}}^i = \frac{1}{\sqrt{2\pi}\sigma_n} \int_{-\infty}^{\eta} \mathrm{e}^{-(\theta^2/2\sigma_n^2) - ((\eta-\theta)^2/2\sigma_1^2)}\,\mathrm{d}\theta \tag{58}$$

$$= \frac{1}{\sqrt{2\pi}\sigma_n} \int_{-\infty}^{\eta} \mathrm{e}^{-\theta^2((1/2\sigma_n^2)+(1/2\sigma_1^2))+(\eta/\sigma_1^2)\theta-(\eta^2/2\sigma_1^2)}\,\mathrm{d}\theta \tag{59}$$

Therefore the detection probability is simplified below

$$P_{\text{d}}^i = \frac{1}{\sqrt{2\pi}\sigma_n} \int_{-\infty}^{\eta} \mathrm{e}^{-b_1^2\theta^2 + b_2\theta - b_3}\,\mathrm{d}\theta \tag{60}$$

where

$$b_1^2 = \frac{1}{2\sigma_n^2} + \frac{1}{2\sigma_1^2} = \frac{1}{2}\left(\frac{1}{\sigma_n^2} + \frac{r_{1i}^2 r_{2i}^2}{v^2\sigma_t^2}\right) \tag{61}$$

$$b_2 = \frac{\eta}{\sigma_1^2} = \frac{\eta r_{1i}^2 r_{2i}^2}{v^2\sigma_t^2} \tag{62}$$

$$b_3 = \frac{\eta^2}{2\sigma_1^2} = \eta\frac{b_2}{2} \tag{63}$$

$$P_{\text{d}}^i = \frac{1}{\sqrt{2\pi}\sigma_n} \int_{-\infty}^{\eta} \mathrm{e}^{-(b_1\theta - (b_2/2b_1))^2 + ((b_2^2/4b_1^2) - b_3)}\,\mathrm{d}\theta \tag{64}$$

$$= \frac{1}{\sqrt{2\pi}\sigma_n} \mathrm{e}^{(b_2^2/4b_1^2)-b_3} \int_{-\infty}^{\eta} \mathrm{e}^{-(b_1\theta - (b_2/2b_1))^2}\,\mathrm{d}\theta \tag{65}$$

By defining u

$$u = b_1\theta - \frac{b_2}{2b_1} \tag{66}$$

P_{d}^i is simplified below

$$P_{\text{d}}^i = \frac{1}{\sqrt{2\pi}\sigma_n b_1} e^{(b_2^2/4b_1^2)-b_3} \int_{-\infty}^{b_1\eta - (b_2/2b_1)} \mathrm{e}^{-u^2}\,\mathrm{d}u \tag{67}$$

$$P_{\text{d}}^i = \frac{1}{\sigma_n b_1} \mathrm{e}^{(b_2^2/4b_1^2)-b_3} \frac{1}{\sqrt{2}} Q\left(\frac{b_2\sqrt{2}}{2b_1} - b_1\eta\sqrt{2}\right) \tag{68}$$

$$= \frac{1}{\sqrt{2}\sigma_n b_1} \mathrm{e}^{(b_2^2/4b_1^2)-b_3} Q\left(\frac{b_2}{b_1\sqrt{2}} - \sqrt{2}b_1\eta\right) \tag{69}$$

From (63), we have

$$P_{\text{d}}^i = \frac{1}{\sqrt{2}\sigma_n b_1} \mathrm{e}^{(b_2/2b_1)^2 - \eta(b_2/2)} Q\left(\frac{b_2}{b_1\sqrt{2}} - \sqrt{2}b_1\eta\right) \tag{70}$$

By substituting the threshold value from (45) instead of η

$$P_{\text{d}}^i = \frac{1}{\sqrt{2}\sigma_n b_1} \mathrm{e}^{(b_2/2b_1)^2 - \sigma_n Q^{-1}(\alpha)(b_2/2)} \times Q\left(\frac{b_2}{b_1\sqrt{2}} - \sqrt{2}b_1\sigma_n Q^{-1}(\alpha)\right) \tag{71}$$

The missed detection probability is also defined as follows

$$P_{\mathrm{M}}^{i} = 1 - P_{\mathrm{d}}^{i} \tag{72}$$

In the following, we will use (3), (72) in order to optimise the positions of the receive antennas and obtain better detection in the whole region of interest.

2.2 Illustrative example

The region of interest is a square with sides equal to 30 km. The configuration of the scenario is shown in Fig. 2. In this scenario, the reference signal is obtained from the transmitter located at $(-6.45, 6.15)$ km, and the Swirling I model [33], with $\sigma_{\mathrm{av}} = 2.4\ \mathrm{m}^2$ is assumed for RCS. In addition, P_{fa} of (45) is set to 10^{-6}.

The parameters of the DVB-T stations and the DVB-T signal used in the correlator are shown in Table 1.

Fig. 3 shows P_{M} for different target's positions in the region of interest. This figure clearly shows the dependence of the P_{M} on the target's position and the geometry of the receive and transmit antennas. The effect of the distance of the target from the transmitters and the receiver on P_{M} is also obvious.

3 P_{M} as a criterion for receive antenna placement

In our simulations, we choose a priority function that defines the value of importance of each location according to the missed probability of the target in that location. In other words, the places with a higher degree of importance are assigned higher values in the priority function so that decreasing missed probability of the target in those places is emphasised more. The priority function chosen in our region of interest is formulated as in (73) and is depicted in Fig. 4.

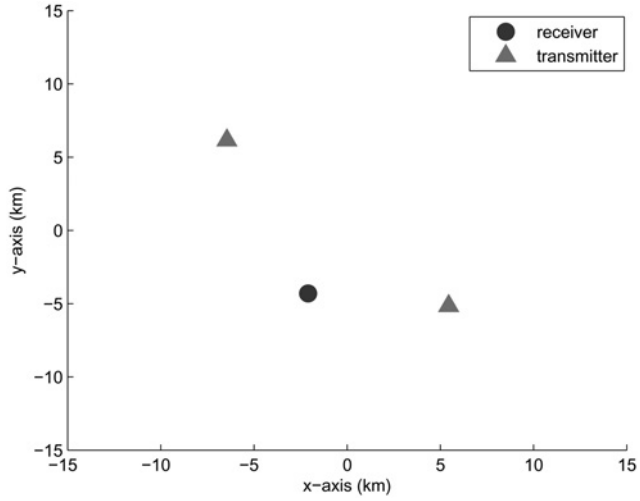

Fig. 2 *Scenario configuration*

Table 1 Simulation parameters

Parameter	Value
P_{T}	1 kW
BW	6 MHz
$G_{\mathrm{T}} = G_{\mathrm{R}}$	0 dB
λ_f	0.6 m
σ_t^2	2.4 m^2
l_{p}	30 dB
NF	7 dB
$L_c L_r$	15 dB
P_{fa}	10^{-6}

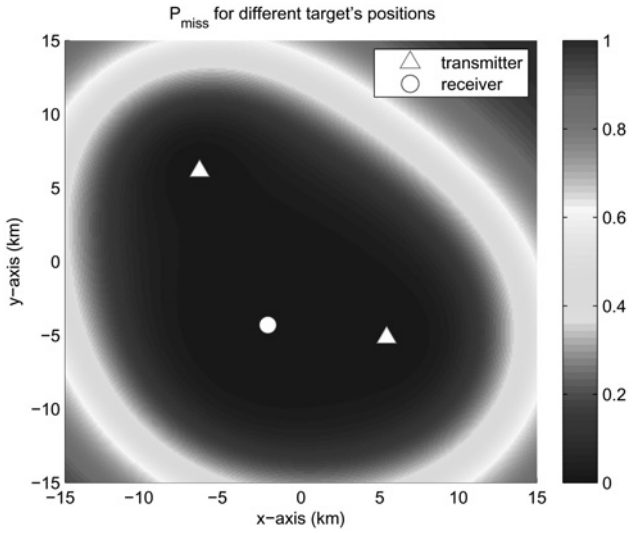

Fig. 3 *P_M for different target's positions*

$$f_{\mathrm{p}}(x, y) = \mathrm{e}^{-(|x-9150|+|y-5350|)/5} + \mathrm{e}^{-(|x+3450|+|y+3550|)/5} \tag{73}$$

It can be inferred that the two locations of (9.15, 5.35) and $(-3.45, -3.55)$ km are of highest priority to detect the targets.

Next, we use the aforementioned probability of missed detection as a criterion to find the best position for placing the receivers. Obviously, for each receiver placement $(\tilde{X})$, P_{M} changes based on where the target is located $(\tilde{Y})$.

Each of the region's positions is a candidate for placing the first receive antenna at that point. Suppose we place the receiver at the point $\tilde{X}$. So, for the position $\tilde{X}$, we can compute output P_{M} of the detector. However, the value of P_{M} changes by changing the position of the target $(\tilde{Y})$.

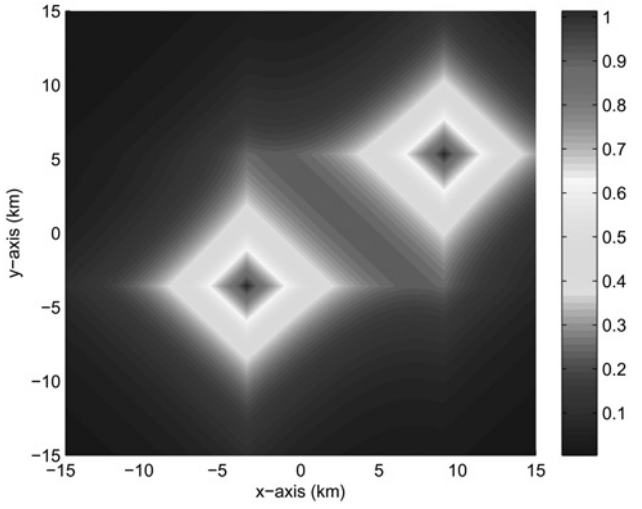

Fig. 4 *Priority function defined in the region of interest*

doi: 10.1049/iet-rsn.2011.0394

Therefore we evaluate the average of the values of P_Ms after changing the target's position ($\tilde{Y}$) in the whole region.

The role of the priority function becomes clear at this stage. Here, before evaluating the average of P_M values, we give the P_M of each location a weight proportional to the value of the priority function at that point. Subsequently, this average P_M can be a criterion of how much $\tilde{X}$ is good for placing the receiver.

Fig. 5 shows the resulting average P_M by changing the receiver's position ($\tilde{X}$) in the whole region. It can be seen from the data of Fig. 5 that the best position of the region to place the receiver is (4.0, 2.3) km, leading to better detection and subsequently, less missed detection.

Fig. 6 shows P_M after placing the receiver at (4.0, 2.3) km for different target positions.

The effect of path loss (raised in $r_{1i}r_{2i}$) is clearly seen in this figure, a factor that is critical to P_M in MIMO localisation. This factor gets more importance as widely separated antennas are used for MIMO localisation and detection. From Fig. 6, it can be noted that as the path from transmitter to target to receiver becomes longer, signal-to-noise ratio values decrease leading to larger values of P_M.

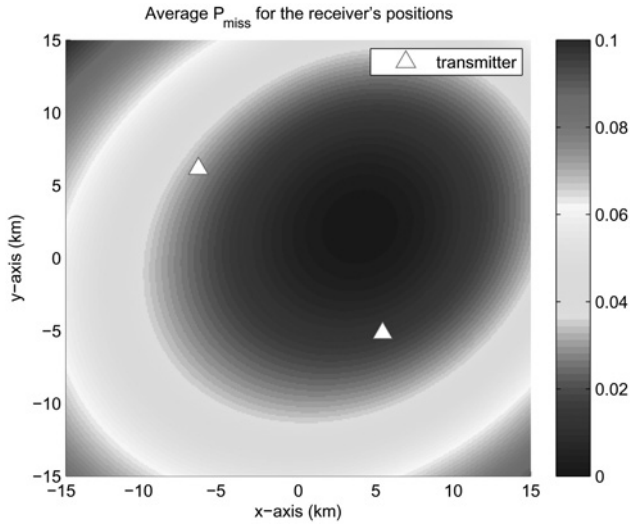

Fig. 5 *Average P_M (weighted by the priority function) obtained by changing the receiver's position*

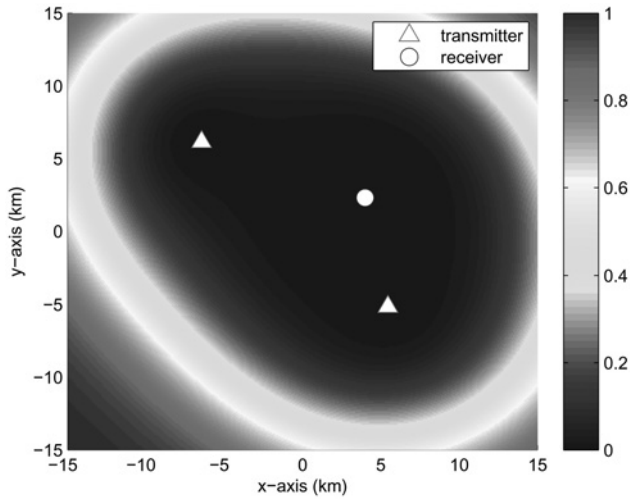

Fig. 6 *P_M obtained for different target positions after placing the first receiver*

4 Improving detection by increasing number of receive antennas

In the next step, we consider the effect of adding the second receive antenna in order to improve the detection performance and do the localisation by jointly processing the two receivers. Our goal is then to find the best position for the second receiver. Using an argument similar to the one presented in the earlier section, we use P_M as the criterion. However, the procedure of finding a good position for the second receiver differs from the earlier case, as will be discussed in the following.

From Fig. 6, it can be seen that after placing the first receiver, high P_Ms at some locations and low P_Ms at others will be observed. Our strategy in placing the second receiver is to complement the coverage of the first receiver. Therefore we choose the second receiver's position such that low P_Ms is obtained at target positions where the first receiver provides a high P_M. Consequently, we can measure the mean P_M at the whole region for placing the second receiver. However, the main difference is that we compute a weighted mean P_M, weighted by the P_Ms obtained from the first receiver (multiplied by the weights resulting from the priority function as given in the previous section). By

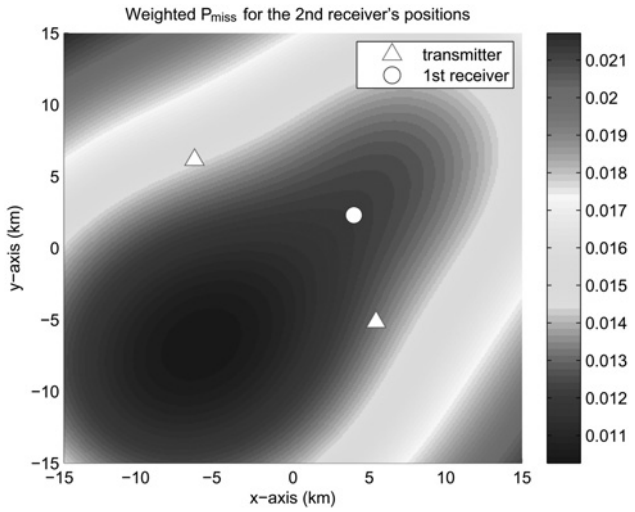

Fig. 7 *Weighted P_M for the second receiver's position*

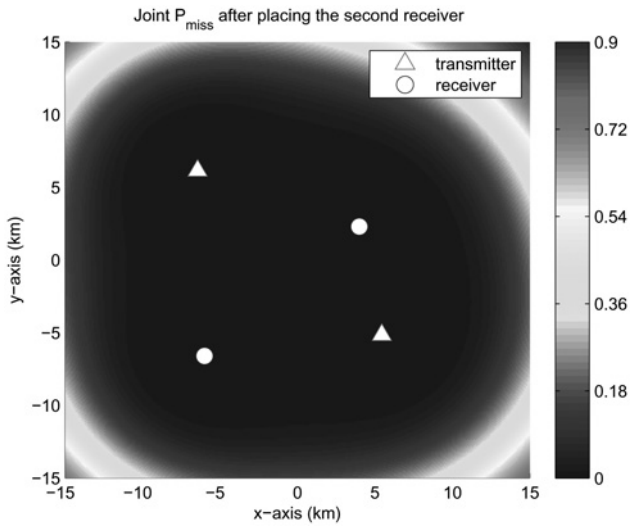

Fig. 8 *Joint P_M after placing the second receiver's position*

computing such weighted mean for the region of interest, we get the P_Ms shown in Fig. 7 for different receiver positions. It can be seen that the best position for the second receiver, by this criterion is $(-6.0, -6.6)$ km.

5 Joint P_M of two receive antennas

Finally, we explore the joint P_M achieved by using both receivers, placed at the positions determined in the previous sections. In this case, the probability of missed detection is obtained in a way similar to the earlier approach, at various target positions. The results are shown in Fig. 8. By comparing this figure with the plot of P_M in the case of only one illuminator (Fig. 6), one can observe the detection's improvement by adding the second receiver.

6 Conclusion

After deriving a closed form for P_M in a MIMO DVB-T-based PCL, we showed that in MIMO PCL schemes we can improve the detection performance by adding more receive antennas. In addition, we showed that this performance critically depends on the geometry of the transmit and receive antennas. As the resulting P_M is highly dependent on the relative position of transmitters, receiver and the object to be localised, it can be a good criterion for choosing the positions of the receive antennas. Since in the PCL case, the illuminators of opportunity are at fixed locations, we introduced this missed detection probability as a criterion for finding the best position for the receiver's antenna. The joint P_M of using two receive antennas in comparison with just using one receiver was also investigated.

7 References

1 Howland, P.E., Maksimiuk, D., Reitsma, G.: 'FM radio based bistatic radar', *IEE Proc. Radar Sonar Navig.*, 2005, **152**, pp. 107–115
2 Lauri, A., Colone, F., Cardinali, R., Bongioanni, C., Lombardo, P.: 'Analysis and emulation of FM radio signals for passive radar'. IEEE Aerospace Conf., 2007, pp. 1–10
3 Di Lallo, A., Farina, A., Fulcoli, R., Genovesi, P., Lalli, R., Mancinelli, R.: 'Design, development and test on real data of an FM based prototypical passive radar'. IEEE Radar Conf., RADAR'08, 2008, pp. 1–6
4 Colone, F., Woodbridge, K., Guo, H., Mason, D., Baker, C.J.: 'Ambiguity function analysis of wireless LAN transmissions for passive radar', *IEEE Trans. Aerosp. Electron. Syst.*, 2011, **47**, (1), pp. 240–264
5 Griffiths, H.D., Long, N.R.W.: 'Television-based bistatic radar', *IEE Proc. F Commun. Radar Signal Process.*, 2008, **133**, (7), pp. 649–657
6 Howland, P.E.: 'Target tracking using television-based bistatic radar', *IEE Proc. Radar Sonar Navig.*, 2002, **146**, pp. 166–174
7 Coleman, C.J., Watson, R.A., Yardley, H.: 'A practical bistatic passive radar system for use with DAB and DRM illuminators'. IEEE Radar Conf., 2008, RADAR'08, 2008, pp. 1–6
8 Radmard, M., Behnia, F., Bastani, M.: 'Cross ambiguity function analysis of the "8 k-mode" DVB-T for passive radar application'. IEEE Radar Conf., 2010, pp. 242–246
9 Saini, R., Cherniakov, M.: 'DTV signal ambiguity function analysis for radar application', *IEE Proc. Radar Sonar Navig.*, 2005, **152**, pp. 133–142
10 Coleman, C., Yardley, H.: 'Passive bistatic radar based on target illuminations by digital audio broadcasting', *IET Radar Sonar Navig.*, 2008, **2**, (5), pp. 366–375
11 Griffiths, H.D., Baker, C.J., Baubert, J., Kitchen, N., Treagust, M.: 'Bistatic radar using satellite-borne illuminators'. RADAR 2002 IEEE, 2003, pp. 1–5
12 Tan, D.K.P., Sun, H., Lu, Y., Lesturgie, M., Chan, H.L.: 'Passive radar using global system for mobile communication signal: theory, implementation and measurements', *IEE Proc. Radar Sonar Navig.*, 2005, **152**, pp. 116–123
13 Sun, H., Tan, D.K.P., Lu, Y.: 'Aircraft target measurements using a GSM-based passive radar'. IEEE Radar Conf., 2008. RADAR'08, 2008, pp. 1–6
14 Sun, H., Tan, D.K.P., Lu, Y., Lesturgie, M.: 'Applications of passive surveillance radar system using cell phone base station illuminators', *IEEE Aerosp. Electron. Syst. Mag.*, 2010, **25**, (3), pp. 10–18
15 Berger, C.R., Demissie, B., Heckenbach, J., Willett, P., Zhou, S.: 'Signal processing for passive radar using OFDM waveforms', *IEEE J. Sel. Top. Signal Process.*, 2010, **4**, pp. 226–238
16 Poullin, D.: 'Passive detection using digital broadcasters (DAB, DVB) with COFDM modulation', *IEE Proc. Radar Sonar Navig.*, 2005, **152**, pp. 143–152
17 Daun, M., Koch, W.: 'Multistatic target tracking for non-cooperative illuminating by DAB/DVB-T'. OCEANS 2007-Europe IEEE, 2007, pp. 1–6
18 Alamouti, S.M.: 'A simple transmit diversity technique for wireless communications', *IEEE J. Sel. Areas Commun.*, 1998, **16**, (8), pp. 1451–1458
19 Haimovich, A.M., Blum, R.S., Cimini, L.J.: 'MIMO radar with widely separated antennas', *IEEE Signal Process. Mag.*, 2007, **25**, (1), pp. 116–129
20 Li, J., Stoica, P.: 'MIMO radar with collocated antennas', *IEEE Signal Process. Mag.*, 2007, **24**, (5), pp. 106–114
21 Lehmann, N.H., Fishler, E., Haimovich, A.M., *et al.*: 'Evaluation of transmit diversity in MIMO-radar direction finding', *IEEE Trans. Signal Process.*, 2007, **55**, (5), pp. 2215–2225
22 Fishler, E., Haimovich, A., Blum, R.S., Cimini, L.J. Jr., Chizhik, D., Valenzuela, R.A.: 'Spatial diversity in radars-models and detection performance', *IEEE Trans. Signal Process.*, 2006, **54**, (3), pp. 823–838
23 Fishler, E., Haimovich, A., Blum, R., Chizhik, D., Cimini, L., Valenzuela, R.: 'MIMO radar: an idea whose time has come'. Proc. IEEE Radar Conf. 2004, 2004, pp. 71–78
24 Li, J., Stoica, P., Xu, L., Roberts, W.: 'On parameter identifiability of MIMO radar', *IEEE Signal Process. Lett.*, 2007, **14**, (12), pp. 968–971
25 Xu, L., Li, J., Stoica, P.: 'Radar imaging via adaptive MIMO techniques'. Proc. 14th European Signal Processing Conf., Florence, Italy, September 2006
26 Fuhrmann, D.R., San Antonio, G.: 'Transmit beamforming for MIMO radar systems using signal cross-correlation', *IEEE Trans. Aerosp. Electron. Syst.*, 2008, **44**, (1), pp. 171–186
27 Stoica, P., Li, J., Xie, Y.: 'On probing signal design for MIMO radar', *IEEE Trans. Signal Process.*, 2007, **55**, (8), pp. 4151–4161
28 San Antonio, G., Fuhrmann, D.R., Robey, F.C.: 'MIMO radar ambiguity functions', *IEEE J. Sel. Top. Signal Process.*, 2007, **1**, (1), pp. 167–177
29 Gumiero, F., Nucciarone, C., Anastasio, V., Lombardo, P., Colone, F.: 'Multistatic passive radar geometry optimization for target 3D positioning accuracy'. European Radar Conf. (EuRAD) IEEE, 2010, pp. 467–470
30 Godrich, H., Haimovich, A.M., Blum, R.S.: 'Target localisation techniques and tools for multiple-input multiple-output radar', *IET Radar Sonar Navig.*, 2009, **3**, (4), pp. 314–327
31 Chitgarha, M.M., Radmard, M., Nazari Majd, M., Nayebi, M.M.: 'Adaptive filtering techniques in passive radar'. 13th Int. Radar Symp. (IRS), 2012, accepted
32 Radmard, M., Karbasi, S.M., Khalaj, B.H., Nayebi, M.M.: 'Data association in multi-input single-output passive coherent location schemes', *IET Radar Sonar Navig.*, 2012, **6**, p. 149
33 Skolnik, M.I.: 'Introduction to radar systems' (McGraw Hill, 1980)

doi: 10.1049/iet-rsn.2011.0394